

Neutron scattering studies in the magnetically dilute kagome staircase system $(\text{Co}_{1-x}\text{Mg}_x)_3\text{V}_2\text{O}_8$

K. Fritsch¹, Z. Yamani², S. Chang³, Y. Qiu^{3,4}, J. R. D. Copley⁴, H. A. Dabkowska⁵, B. D. Gaulin^{1,5,6}

¹ Department of Physics and Astronomy, McMaster University, Hamilton, Ontario, L8S 4M1, Canada

² National Research Council, Canadian Neutron Beam Centre, Chalk River, ON, Canada

³ NIST Center for Neutron Research, NIST, Gaithersburg, Maryland 20899-8102, USA

⁴ Department of Materials Science and Engineering, University of Maryland, College Park, Maryland 20742, USA

⁵ Brockhouse Institute for Materials Research, Hamilton, Ontario, L8S 4M1, Canada

⁶ Canadian Institute for Advanced Research, 180 Dundas St. W., Toronto, Ontario, M5G 1Z8, Canada

Geometrically frustrated materials that are based on magnetic moments that decorate a lattice of triangular networks have been of great recent interest due to their intriguing low-temperature magnetic properties and a rich variety of exotic ground states such as spin glasses, spin ices, and spin liquids [1]. Perhaps the best known geometrically frustrated structure is the two-dimensional Kagome lattice which consists of antiferromagnetically coupled spins situated on a network of corner-sharing equilateral triangles.

$\text{Co}_3\text{V}_2\text{O}_8$ belongs to the $\text{M}_3\text{V}_2\text{O}_8$ family ($\text{M}=\text{Co}, \text{Ni}, \text{Cu}, \text{Mn}$) which represents an anisotropic variation of the ideal Kagome lattice. In this structure 3d-transition metal M^{2+} ions decorate kagome layers that are buckled in and out of the plane forming the so-called kagome staircase. In particular, $\text{Co}_3\text{V}_2\text{O}_8$ crystallizes in an orthorhombic crystal structure with space group Cmca , in which edge-sharing Co^{2+}O_6 octahedra (shown in red and blue in figure 1a) are situated slightly below and above the a-c plane to form the kagome staircase. These buckled layers are stacked along the crystallographic b-axis and are separated by non-magnetic V^{5+}O_4 tetrahedra (shown in pink). Within the a-c plane (figure 1b), the kagome layers are composed of $S=3/2$ magnetic moments that reside on two crystallographically inequivalent Co^{2+} sites, with crystallographic (4a) cross-tie sites (red) linking (8c) spine sites (blue) that form chains along the a-axis.

The low-temperature magnetic phase diagrams of all known members of the kagome staircase family are fairly complex and differ considerably, despite their isostructurality. For example, $\text{Ni}_3\text{V}_2\text{O}_8$ displays four different magnetically ordered states below 10 K and has attracted much interest due to the discovery of multiferroicity in one of its incommensurate phases at low temperatures [2]. The phase diagram of $\text{Co}_3\text{V}_2\text{O}_8$ has been studied by neutron diffraction, dielectric and magnetization measurements [3,4] revealing a series of five different magnetic phase transitions upon cooling below 11.2 K that ultimately culminate in a simple ferromagnetic ground state below $T \sim 6.1$ K. All five of the magnetic states display a preferred direction of the spins parallel to the a-axis. The excitation spectrum out of the ferromagnetic ground state has been measured on a large, high-quality single crystal using inelastic neutron scattering techniques and has been described by linear spin-wave theory and a simple model Hamiltonian [5]. The results give a weak magnetic superexchange coupling of $J_{\text{sc}} \sim 15$ K between the spine and cross-tie sites in the kagome plane while showing that, surprisingly, the magnetic coupling between adjacent spine sites can be neglected.

In the present study, we investigated the effect of site disorder on the ferromagnetic ground state and its low-lying excitations by introducing quenched impurities in the form of non-magnetic Mg^{2+} ions that substitute for magnetic Co^{2+} . To that end, two large (4-5g) high-quality single crystals of $(\text{Co}_{1-x}\text{Mg}_x)_3\text{V}_2\text{O}_8$ with Mg^{2+} concentrations of $x = 0.05$ and $x = 0.20$ were grown at McMaster University using an optical floating-zone image furnace. Details of these growths and results of X-ray structural refinements will be published elsewhere [6]. We find that the site dilution of the magnetic Co^{2+} ions by non-magnetic Mg^{2+} is almost perfectly random.

Magnetization measurements were performed along different crystallographic axes on both samples. The results are presented in figure 2. These measurements show a lowering of the ferromagnetic transition temperature from $T_{\text{C}} \sim 6.1$ K in the pure material to $T_{\text{C}} \sim 5.2$ K in the $x = 0.05$ sample (filled circles), while the phase transition is completely absent in the $x = 0.20$ Mg^{2+} -doped sample (open circles) down to the lowest accessible temperature in our SQUID setup ($T \sim 2$ K). This result is somewhat unexpected since the doping level is much lower than the theoretical percolation threshold which is about $x \sim 0.5$ for the destruction of long range order in a two-dimen-

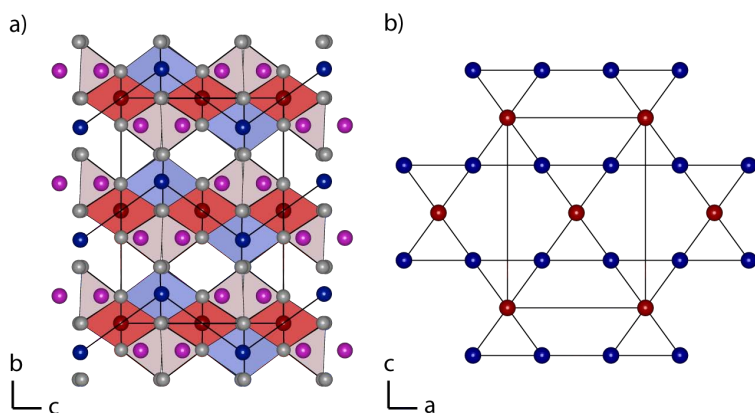


Fig 1. Crystal structure of $\text{Co}_3\text{V}_2\text{O}_8$. a) View of the kagome staircase formed by Co^{2+}O_6 octahedra (red and blue) which are stacked along the b-axis separated by non-magnetic V^{5+}O_4 tetrahedra (pink). b) View of the kagome plane projected on the a-c plane with the crystallographically inequivalent cross-tie (red) and spine sites (blue).

sional system and $x \sim 0.7$ in a three-dimensional system. This indicates that the response of this system to disorder is more sophisticated than one would guess for a simple ferromagnetic percolation problem.

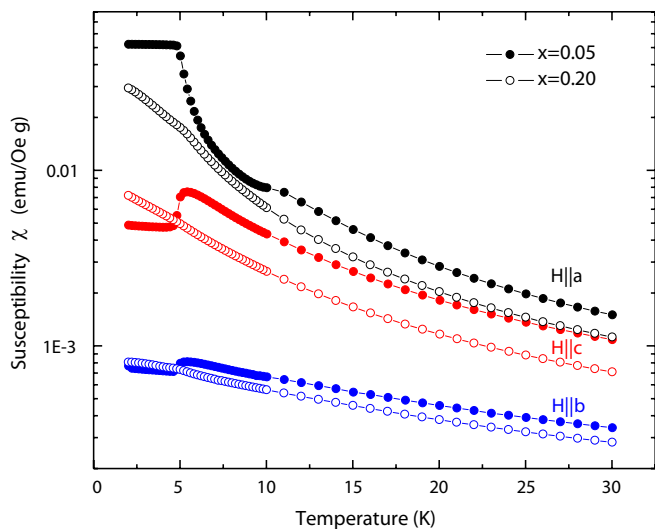


Fig 2. Magnetic susceptibility measurements at an applied field of $H = 50$ Oe along the three crystallographic axes for $(\text{Co}_{1-x}\text{Mg}_x)_3\text{V}_2\text{O}_8$ with $x = 0.05$ (filled circles) and $x = 0.20$ (open circles).

We performed elastic and inelastic neutron scattering measurements to probe the nature of the static and dynamic correlations in both crystals within the kagome plane. The crystals were therefore oriented in the $(H,0,L)$ scattering plane. Elastic neutron scattering measurements on the $x = 0.20$ Mg doped sample were carried out on the C5 triple-axis spectrometer at the NRU reactor. Vertically-focussing pyrolytic graphite PG-002 monochromator and flat PG-002 analyzer crystal were used. The measurements were performed at a fixed final neutron energy of $E_f = 14.7$ meV, with a collimation of $[none, 0.477^\circ, 0.55^\circ, 1.2^\circ]$. Two PG filters were placed in the scattered beam to eliminate higher order wavelength contamination of the beam. Before the unscheduled shutdown of the NRU reactor, we were able to follow the temperature dependence of the elastic magnetic scattering around the $(0,0,2)$ Bragg peak, which is a weak nuclear but a strong ferromagnetic Bragg peak in the pure material. Figure 3 shows that, in agreement with the magnetization data, no magnetic long range order is present down to ~ 3 K, however very broad diffuse scattering around the $(0,0,2)$ reciprocal lattice point is observed (not observed in pure $\text{Co}_3\text{V}_2\text{O}_8$), indicating the presence of extremely short-ranged correlations in the material. The diffuse scattering feature decreases with increasing temperature and has almost completely vanished at $T \sim 10$ K as shown in the inset of figure 3.

We further studied the elastic scattering of both diluted $(\text{Co}_{1-x}\text{Mg}_x)_3\text{V}_2\text{O}_8$ crystals on the cold triple-axis spectrometer SPINS at the NCNR at NIST. These measurements employed a vertically focussing PG-002 monochromator and flat PG-002 analyzer crystal with a fixed final energy of $E_f = 5$ meV. The collimating settings were $[open, 80', 80', 80']$ with an

in-pile cooled Be filter placed in the diffracted beam incident to the sample. The samples were placed in an Orange cryostat with a base temperature of 1.5 K.

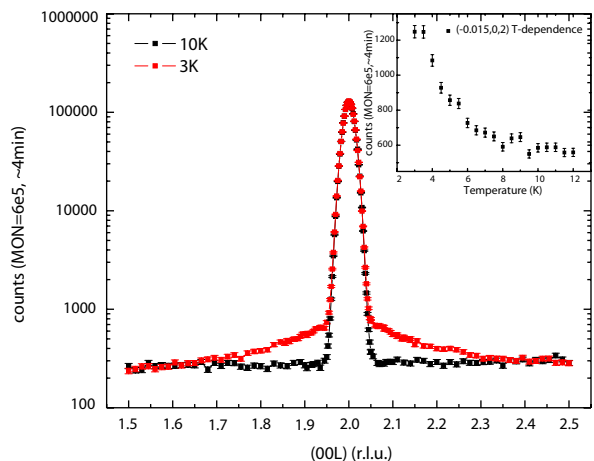


Fig 3. Observed elastic magnetic scattering around the $(0,0,2)$ Bragg peak for $(\text{Co}_{1-x}\text{Mg}_x)_3\text{V}_2\text{O}_8$ with $x = 0.20$ showing broad diffuse scattering at 3 K. The inset shows the temperature evolution of the diffuse scattering at the $(-0.015, 0, 2)$ position.

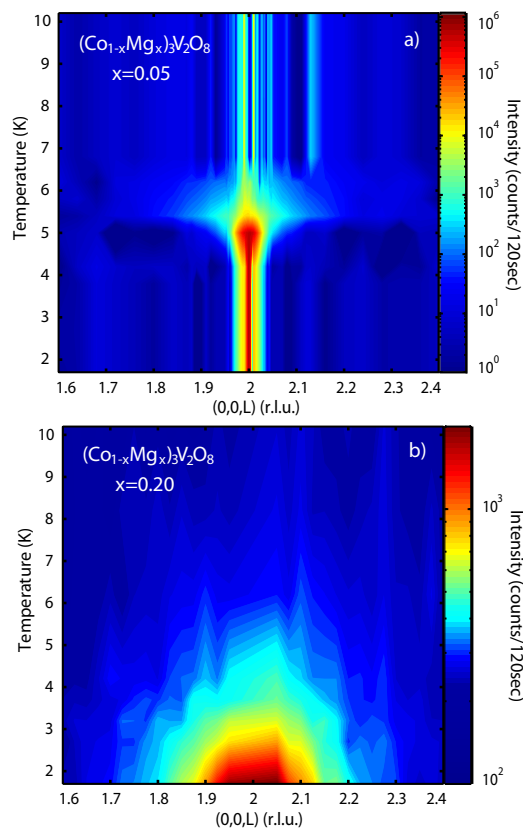


Fig 4. Contour plots showing the temperature evolution of the elastic magnetic scattering around the $(0,0,2)$ Bragg peak position for a) $x = 0.05$ and b) $x = 0.20$. Note that the intensity of the weak nuclear $(0,0,2)$ Bragg peak at 20 K has been subtracted from the individual $(0,0,L)$ scans making up the contour plots, which leads to artefacts around the $(0,0,2)$ position at higher temperatures in panel a) for $x = 0.05$.

The results of elastic $(0,0,L)$ scans as a function of temperature for both samples are presented as color contour plots in figure 4a) and b). In both data sets shown, the high temperature data at $T = 20$ K is used to subtract the nuclear scattering and hence to isolate the magnetic scattering. It can easily be seen that the scattering profiles for the two samples are in striking contrast to each other.

As the temperature is lowered below $T \sim 7$ K in the $x = 0.05$ Mg-doped sample (figure 4a)), diffuse scattering intensity characteristic of the development of short range correlations builds up and increases down to a temperature of $T \sim 5.4$ K below which it gives way to a sharp increase in scattering intensity at the $(0,0,2)$ position associated with the first-order transition to the ferromagnetic ground state.

Interestingly, the short range correlations get really pronounced below a temperature of $T \sim 6.5$ K, which roughly coincides with the ordering temperature in pure $\text{Co}_3\text{V}_2\text{O}_8$. This suggests that the magnetic moments in the doped material somehow "know" at which temperature they should order. The $(0,0,L)$ scans in this sample are best described by a two-

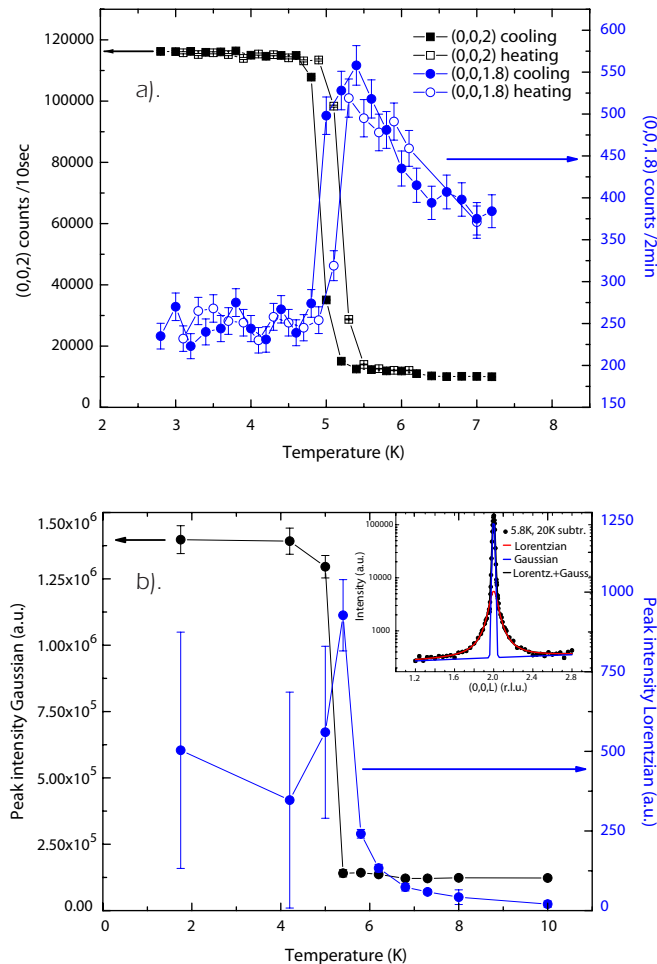


Fig 5. a) Order parameter and diffuse scattering near $(0,0,2)$ shown as a function of temperature for $x = 0.05$. b) Data for $x = 0.05$ fit to a sum of Gaussian and Lorentzian lineshapes. The inset shows a repre-

sentative scan at 5.8 K. The evolution of the diffuse scattering and the ferromagnetic Bragg peak intensity are shown quantitatively in figure 5a).

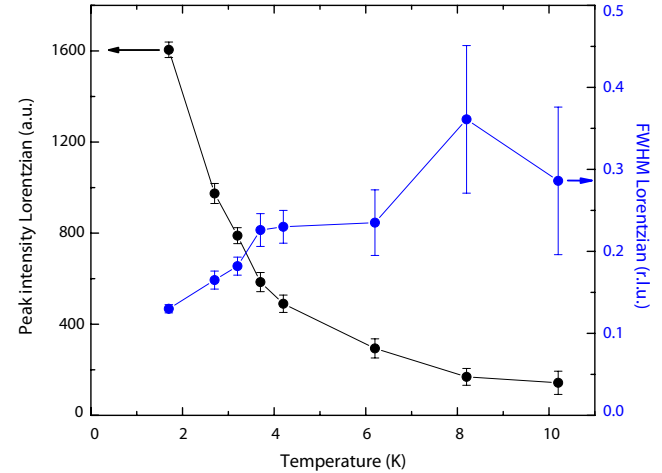


Fig 6. Results of a Lorentzian lineshape fitting of the elastic scattering in $(\text{Co}_{1-x}\text{Mg}_x)_3\text{V}_2\text{O}_8$ with $x = 0.20$.

In contrast to the $x = 0.05$ doped sample, the $x = 0.20$ Mg-doped crystal fails to enter a long range ordered state at least down to the base temperature of 1.5 K, consistent with the magnetization measurements. The scattering profile is entirely dominated by broad diffuse scattering intensity that develops noticeably below ~ 6 K increasing monotonically on cooling down to 1.5 K. The scattering intensities can be described by a single-component Lorentzian lineshape for all temperatures as shown in figure 6. From the FWHM of the Lorentzian, a real-space correlation length of the spins within the kagome plane of about 10\AA can be extracted, which corresponds roughly to the size of one unit cell. This confirms the extreme short range nature of the correlations in this sample.

In addition to the study of the elastic scattering, we investigated the evolution of the dynamic correlations (the excitations out of the ground state) through inelastic neutron scattering measurements. For this purpose, we used the time-of-flight instrument DCS at the NCNR at NIST employing a fixed incident wavelength of $\lambda_i = 2.5\text{\AA}$ to access magnetic excitations up to energy transfers of $\Delta E \sim 10$ meV. Figure 7 shows the scattering observed at 1.5 K for both $x = 0.05$ (panels a) and b)) and $x = 0.20$ (panels c), d)) samples.

In particular, the cuts along the H- or L-directions in figure 7 were taken by integrating over a narrow range in L and H ($H, L = [-0.05, 0.05]$) to enable the comparison with previous data obtained for the pure sample using a triple-axis instrument (see Ramazanoglu et al. [5]). The $x = 0.05$ Mg-doped sample exhibits two spin-wave branches, one at low energy ~ 2 meV and one at higher energies ~ 4 -6 meV with a finite lifetime. The dispersion of the spin excitations in the pure

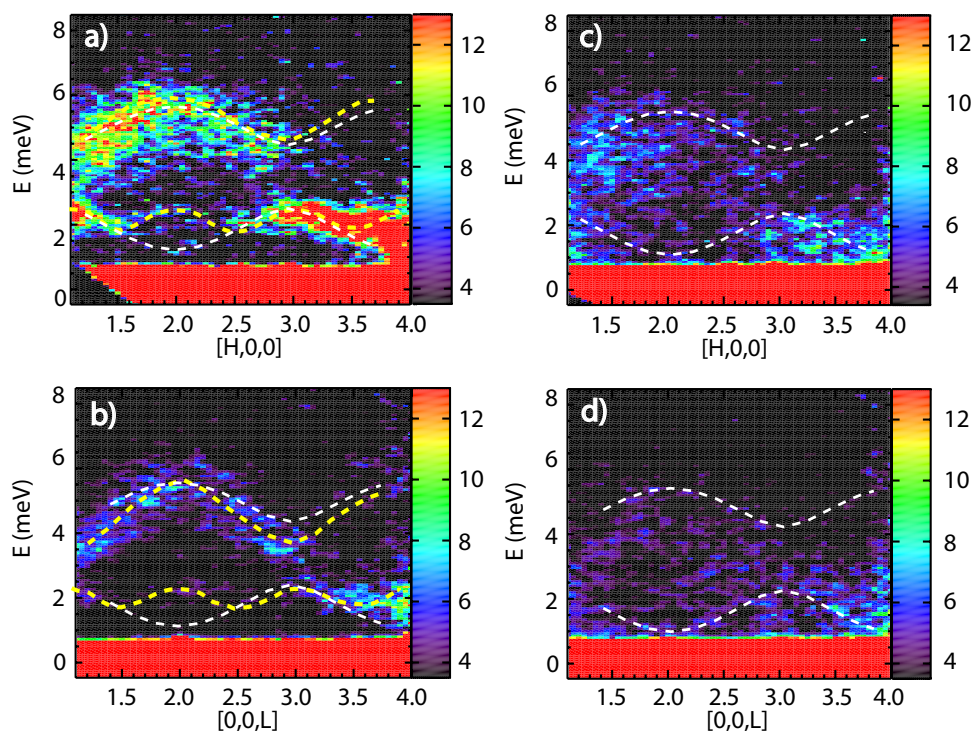


Fig 7. Excitation spectrum at 1.5 K for $x = 0.05$ (panels a) and b)) and $x = 0.20$ (panels c) and d)) along two different directions in reciprocal space. The white lines indicate the calculated spin-wave dispersion for the pure material [5], while the yellow lines serve as a guide to the eye.

sample, derived from spin wave theory, is shown in white. We see that both the pure and $x = 0.05$ Mg-doped samples possess qualitatively similar excitation spectra in their ordered states. However, the description based on the linear spin-wave theory is not perfect, as the lower energy spin-wave branch seems to follow a dispersion that differs from the calculated theoretical one. The inelastic scattering for the $x = 0.20$ Mg-doped sample does not show evidence for distinct spin-wave excitations but exhibits diffuse scattering, as expected from the absence of a long range ordered state in this material at 1.5 K.

In conclusion, we have performed elastic and inelastic neutron scattering measurements on two single crystal samples of the magnetically dilute kagome staircase material $(\text{Co}_{1-x}\text{Mg}_x)_3\text{V}_2\text{O}_8$ with $x = 0.05$ and $x = 0.20$. We found that, in contrast to expectations from percolation theory, a surprisingly small amount of site disorder at the $x = 0.05$ and $x = 0.20$ doping levels is sufficient to dramatically influence the magnetic order at low temperatures. The ferromagnetic transition temperature is suppressed by almost 20% from the pure material for a doping level of $x = 0.05$ while a doping level of $x = 0.20$ causes the material to remain in an extremely short range correlated state down to the lowest temperatures measured (~ 1.5 K). The excitation spectrum for the $x = 0.05$ doped material shows good, albeit not perfect agreement with expectations and theoretical calculations derived from the pure material. Further quantitative analysis of the data is required to derive more quantitative results and to understand this material in more detail.

References

- [1] Frustrated Spin Systems, edited by H.T. Diep (World Scientific Publishing Co. Pte. Ltd., Singapore, 2004)
- [2] G. Lawes, M. Kenzelmann, N. Rogado, K. H. Kim, G. A. Jorge, R. J. Cava, A. Aharony, O. Entin-Wohlman, A. B. Harris, T. Yildirim, Q. Z. Huang, S. Park, C. Broholm, and A. P. Ramirez, *Phys. Rev. Lett.* **93**, 247201 (2004).
- [3] Y. Chen, J. W. Lynn, Q. Huang, F. M. Woodward, T. Yildirim, G. Lawes, A. P. Ramirez, N. Rogado, R. J. Cava, A. Aharony, O. Entin-Wohlman, and A. B. Harris, *Phys. Rev. B* **74**, 014430 (2006).
- [4] R. Szymczak, M. Baran, R. Diduszko, J. Fink-Finowicki, M. Gutowska, A. Szewczyk, and H. Szymczak, *Phys. Rev. B* **73**, 094425 (2006).
- [5] M. Ramazanoglu, C. P. Adams, J. P. Clancy, A. J. Berlinsky, Z. Yamani, R. Szymczak, H. Szymczak, J. Fink-Finowicki, and B. D. Gaulin, *Phys. Rev. B* **79**, 024417 (2009).
- [6] K. Fritsch, M. Ramazanoglu, H. A. Dabkowska, and B. D. Gaulin (to be published)